JOURNAL OF GEOPHYSICAL RESEARCH, VOL. 113, A05221, doi:10.1029/2007JA012744, 2008

Click Here for Full Article

Interplanetary conditions causing intense geomagnetic storms (Dst ≤ -100 nT) during solar cycle 23 (1996–2006)

E. Echer,[1] W. D. Gonzalez,[1] B. T. Tsurutani,[2] and A. L. C. Gonzalez[1]

Received 21 August 2007; revised 24 January 2008; accepted 8 February 2008; published 30 May 2008.

[1] The interplanetary causes of intense geomagnetic storms and their solar dependence occurring during solar cycle 23 (1996–2006) are identified. During this solar cycle, all intense (Dst ≤ -100 nT) geomagnetic storms are found to occur when the interplanetary magnetic field was southwardly directed (in GSM coordinates) for long durations of time. This implies that the most likely cause of the geomagnetic storms was magnetic reconnection between the southward IMF and magnetopause fields. Out of 90 storm events, none of them occurred during purely northward IMF, purely intense IMF *By* fields or during purely high speed streams. We have found that the most important interplanetary structures leading to intense southward *Bz* (and intense magnetic storms) are magnetic clouds which drove fast shocks (sMC) causing 24% of the storms, sheath fields (Sh) also causing 24% of the storms, combined sheath and MC fields (Sh+MC) causing 16% of the storms, and corotating interaction regions (CIRs), causing 13% of the storms. These four interplanetary structures are responsible for three quarters of the intense magnetic storms studied. The other interplanetary structures causing geomagnetic storms were: magnetic clouds that did not drive a shock (nsMC), non magnetic clouds ICMEs, complex structures resulting from the interaction of ICMEs, and structures resulting from the interaction of shocks, heliospheric current sheets and high speed stream Alfvén waves. During the rising phase of the solar cycle, sMC and sheaths are the dominant structure driving intense storms. At solar maximum, sheath fields, followed by Sh+MCs and then by sMC were responsible for most of the storms. During the declining phase, sMC, Sh and CIR fields are the main interplanetary structures leading to intense storms. We have also observed that around 70% of the storms follow the interplanetary criteria of $Ey \geq 5$ mV/m for at least 3 h. Around 90% of the storms used in the study followed a less stringent set of criteria: $Ey \geq 3$ mV/m for at least 3 h. Finally, we obtain the approximate rate of intense magnetic storms per solar cycle phases: minimum/rising phase 3 storms.year^{-1}, maximum phase 8.5 storms.year^{-1}, and declining/minimum phases 6.5 storms.year^{-1}.

Citation: Echer, E., W. D. Gonzalez, B. T. Tsurutani, and A. L. C. Gonzalez (2008), Interplanetary conditions causing intense geomagnetic storms (Dst ≤ -100 nT) during solar cycle 23 (1996–2006), *J. Geophys. Res.*, *113*, A05221, doi:10.1029/2007JA012744.

1. Introduction

[2] Geomagnetic storms are magnetospheric disturbances that have been studied for more than 200 years [*Gonzalez et al.*, 1994; *Tsurutani et al.*, 1997 and references therein]. They are characterized by enhanced particle fluxes in the radiation belts. The enhanced fluxes can be indirectly measured by decreases in the Earth's magnetic field horizontal component caused by the diamagnetic effect generated by the ring current. A standard measure of this is the *Dst* index, which is proportional to the total kinetic energy of ~20–200 keV particles within the outer radiation belt, thus it is a good quantitative measure of the intensity of the geomagnetic storm. The inner edge of the ring current is located at 4 R_E or less from the Earth's surface during intense storms. For lesser intensity storms, the ring current is located further away from the Earth [*Gonzalez et al.*, 1994; *Daglis et al.*, 1999].

[3] Several mechanisms have been suggested to explain geomagnetic storms as the result of an enhanced solar wind-magnetosphere energy coupling process. Among them, two leading candidates are "viscous interaction" [*Axford and Hines*, 1961] and magnetic reconnection [*Dungey*, 1961]. In the first mechanism, the solar wind flowing past the Earth's magnetopause has a viscous interaction causing energy transfer from the solar wind to the magnetosphere. The

[1] Instituto Nacional de Pesquisas Espaciais (INPE) – POB 515, Sao Jose dos Campos, Sao Paulo, Brazil.
[2] Jet Propulsion Laboratory (JPL), California Institute of Technology, Pasadena, California, USA.

Copyright 2008 by the American Geophysical Union.
0148-0227/08/2007JA012744$09.00

Kelvin-Helmholtz instability in particular, has been widely studied as a specific type of viscous interaction.

[4] The magnetic reconnection mechanism/model consists of fusion/merging of oppositely directed magnetic field lines, with the net result being the conversion of magnetic energy in heating and acceleration of the plasma. The change in magnetic connection or topology is a profound effect, allowing previously unconnected regions to exchange plasma and mass/momentum/energy [*Hughes*, 1995]. In the case of Earth's magnetosphere, the dayside geomagnetic field is northward directed in GSM coordinates, so magnetic reconnection is more effective when the IMF *Bz* is southwardly (*Bs*) directed [*Dungey*, 1961].

[5] Another mechanism proposed in the literature is cross-field diffusion from the magnetosheath to the magnetopause boundary layers by resonant wave-particle interactions [e.g., *Tsurutani and Thorne*, 1982]. For a limited number of events, *Tsurutani and Gonzalez* [1995] investigated the solar wind–magnetosphere energy coupling during intervals with IMF $Bz > 0$. They found that the energy transfer efficiency from the solar wind to the magnetosphere for viscous interaction or magnetospheric reconnection during these northward IMF intervals was a maximum of 1/100 to1/30 that of IMF $Bz < 0$ intervals.

[6] The subject of the solar and interplanetary origin of geomagnetic storms has been widely studied [e.g., *Gonzalez et al.*, 1999; *Zhang et al.*, 2007, and references therein]. *Tsurutani et al.* [1988] studied the interplanetary causes of intense geomagnetic storms ($Dst \leq -100$ nT) for the peak year of the maximum phase of solar cycle 21 (1978–1979) and found that about half of the storms were associated with magnetic clouds (MCs), as defined by *Burlaga et al.* [1981], and half with sheath field (Sh) regions (following interplanetary shocks). Sheath fields/plasmas are the compressed solar wind downstream of interplanetary shocks. In all cases of this study, the pertinent shocks were driven by fast ICMEs at 1 AU. *Tsurutani et al.* [1992] and *Echer et al.* [2008] studied "great storms" with $Dst < -250$ nT and found about the same relative ratios. Many authors have studied the geoeffectiveness of interplanetary structures (see for example the review of *Gonzalez et al.* [1999], and the recent work of *Zhang et al.* [2007]). Several studies have been done concerning the solar origin of ICMES leading to storms (e.g., references by *Schwenn* [2006] and *Zhang et al.* [2007]). We refer the interested reader to these articles.

[7] *Gonzalez et al.* [2007] made a previous study of the interplanetary origin of intense geomagnetic storms during solar cycle 23. They found that the most common interplanetary structures leading to the development of an intense storm were: ICMEs containing a MC topology, sheath fields, sheath fields followed by a magnetic cloud and corotating interaction regions leading high speed streams. However, the relative importance of each of those driving structures was found to vary with the phase of the solar cycle.

[8] The purpose of the present paper is to study all intense geomagnetic storms ($Dst \leq -100$ nT) that occurred during 1996–2006, during solar cycle 23. All 90 storms that occurred during the 11 year (half the 22 year Hale) sunspot cycle were studied in detail using high time resolution interplanetary plasma and magnetic field data. We considered the following candidates as possible interplanetary drivers of the storm main phase: sheath magnetic fields, magnetic cloud fields, ICMEs non-magnetic cloud (nonMC) fields, CIRs, high speed streams, Alfvén wave fluctuations, shock compressions, and heliospheric current sheet crossings. Combinations of all of the above were also investigated. Many of these interplanetary phenomena have been previously proposed/identified as candidates for solar wind energy transfer mechanisms. It is clear that solar wind energy transfer to the magnetosphere does occur during these phenomena, but at what level? How important are they for the generation of intense geomagnetic storms? Magnetic reconnection of northward IMF fields can occur at the cusp [*Smith and Lockwood*, 1996], but is it possible that the energy input flows to the distant tail and not to the magnetosphere? Recently several excellent examples of Kelvin Helmholtz waves at the tail flanks have been noted to occur during high speed streams with northward IMFs [e.g., *Fairfield et al.*, 2003], but can these events cause intense geomagnetic storms? It has also been surmised that sector boundary crossings may cause geomagnetic activity enhancements [*Schatten and Wilcox*, 1967]. Is it the sector boundary themselves or adjacent CIRs as suggested by *Tsurutani et al.* [1995] that are responsible for the energy transfer? Is the energy transfer intense enough to create an intense magnetic storm? Finally, it has been shown by *Hudson et al.* [1997] that the interplanetary shocks in the presence of solar flare particles entering the magnetosphere can lead to the formation of new radiation belts. These observations are robust and modeling has confirmed the mechanism. However, can shocks alone (without IMF Bs fields) create major geomagnetic storms? *Garrett* [1974] found a relationship between highly fluctuating interplanetary magnetic fields (IMFs) and geomagnetic activity. The suggested mechanism was one of viscous interaction between the interplanetary turbulence and the magnetopause. However, in the studied cases, the IMF fluctuations led only to substorm activity. Can such interactions cause intense geomagnetic storms? One of the purposes of our study will be to identify intense geomagnetic storms (if any) that are caused by features other than magnetic reconnection due to southward IMFs.

2. Methodology

2.1. Interplanetary Terminology

[9] There has been some confusion in the interplanetary and solar terminology related to magnetic storms [*Schwenn*, 1996; *Burlaga*, 2001; *Russell*, 2001]. Thus we will give a brief review of terminology to attempt to remove any possible confusion. The solar wind has three basic types of flows: the background (slow) solar wind, (emitted from regions in or around helmet streamers), transient ejecta, and high speed flows from coronal holes [*Burlaga*, 1995]. Transient ejecta and coronal hole high-speed streams (and their interaction with the background slow solar wind) can be geoeffective if they contain a significant southward directed IMF *Bz* component. This would be in agreement with the magnetic reconnection mechanism.

[10] When coronal holes evolve/expand to reach low heliographic latitudes, the fast streams emanating from them can intercept the Earth. As these fast streams overtake the background (slow) solar wind, an interaction region is

formed. This interaction forms a compression region between the high speed stream and slow speed stream [*Burlaga and Ogilvie*, 1970; *Balogh et al.*, 1999]. The front portion is the slow solar wind that has been heated (compressed) and accelerated. The trailing (sunward) portion is the fast solar wind that has been compressed and decelerated. When coronal holes are long-lived, these streams will recur every ~27 days. The term interaction region was introduced by *Burlaga and Ogilvie* [1970] referring to regions of high pressure generated by fast flows, transient or corotating. The subset of interaction regions associated with long-lived corotating streams was called CIRs by *Smith and Wolfe* [1976]. Because CIRs are intense magnetic field regions, they can cause magnetic storms if the fields are directed southward. Since CIRs are not fully developed by 1 AU, some authors have called them proto-CIRs [*Gonzalez et al.*, 1999].

[11] The transient solar wind consists of the material emitted during coronal mass ejections (CMEs) that propagates into interplanetary space. CMEs are the outward expulsion of large amount of solar and coronal mass and they are observed with instruments such as coronagraphs [*Hundhausen*, 1972; *Gosling*, 1997; *Schwenn*, 2006]. A CME viewed near the sun has 3 fundamental components: the bright outer loops, a dark region and a filament [*Hundhausen et al.*, 1984; *Schwenn*, 2006]. However, farther from the sun (at 1 AU), CMEs are no longer visible and only plasma and magnetic field measurements are available to identify these features. In addition, CMEs may have become highly distorted as they propagate through interplanetary space. Some CME parts may separate or even fall back into the sun.

[12] The interplanetary remnants of CMEs have been called driver gases, ejecta, interplanetary coronal mass ejections (ICMEs), among other names [*Tsurutani et al.*, 1997]. A component of an ICME with special characteristics is a magnetic cloud (MC). *Burlaga* [1995] and *Burlaga et al.* [1981] defined MCs by two criteria: strong magnetic fields, and a smooth rotation of the field direction through a large angle, close to 180°. Other criterion used to define MC is a low proton temperature/low beta.

[13] One ongoing research topic is what portion of a CME does the 1 AU plasma driver gas/MC components correspond to? It is believed that the MC is the dark void portion of the CME [*Farrugia et al.*, 1997; *Tsurutani and Gonzalez*, 1997]. The low plasma beta and low temperatures of the MC are consistent with a lower level of light scattering near the Sun. A strong magnetic field is present within the region to preserve pressure balance. If this is the case, then a pertinent question is "what has happened to the other portions of the CME, the bright outer loops and the filament?" The 10–11 January 1997 event is one of the rare cases where all three CME components have been identified at 1 AU. *Tsurutani et al.* [1998] identified plasma features that have been interpreted as the interplanetary signatures of the bright loops. *Burlaga et al.* [1998] identified interplanetary features that were interpreted as a high density filament.

[14] When an ICME has a speed that is greater than the upstream plasma speed by a value that is more than Vms (Vms is the upstream magnetosonic speed), a fast forward interplanetary shock will form. The shock will expand outward from the CME forming a "sheath", a region where highly turbulent solar wind plasma and fields are observed [*Kennel et al.*, 1985; *Tsurutani et al.*, 1988].

2.2. Data Analysis

[15] In this paper we have used the *Dst* data, provided by the World Data Center for Geomagnetism, Kyoto (http://swdcdb.kugi.kyoto-u.ac.jp/) and the interplanetary data observed by the ACE and WIND satellites. During solar cycle 23 (1996–2006), 90 intense storms ($Dst \leq -100$ nT) have been identified and investigated in detail. These storms are listed in Table 1. The columns in Table 1 are: the date of peak *Dst*, the value of peak *Dst* and the interplanetary structure identified as the cause of the storm main phase. Table 2 shows the interplanetary causes of geomagnetic storms for each year of cycle 23.

[16] For the identification of the interplanetary causes we have followed the nomenclature and definitions given by *Burlaga et al.* [1981], *Tsurutani et al.* [1988, 1995], *Gonzalez et al.* [1999], and *Balogh et al.* [1999] and presented in the previous section. In this paper we use the following definitions:

[17] - CIRs: correspond to the interaction regions between high and low speed solar wind streams.

[18] - Sheath (Sh): fields present in the region between the interplanetary shock and the driver ICME.

[19] - MC: a subset of the ICMEs that follow the 3 MC criteria stated above. In this paper, we have considered an ICME to be a MC only when the *Bz* or *By* magnetic field component displayed a ~180° rotation. Note that other authors used slightly different criteria for MCs [e.g., *Huttunen et al.*, 2005; *Zhang et al.*, 2007].

[20] - When the MC was preceded by an interplanetary fast shock, but only the MC field caused the storm, we called this type of event a MC with a shock (sMC). When the MC was not preceded by an interplanetary shock, we called this event a MC with no shock (nsMC).

[21] - nonMC: any ICME that does not follow the MC criteria: low plasma beta, high magnetic fields and a full, ~180° rotation in *By* or *Bz* component.

[22] Other designations in the table are: "Sh+MC" for a sheath followed by a MC, "SBC" for a sector boundary crossing, "S compr MC" for a magnetic cloud compressed by a shock, and "Complex" for a case in which there is a combination/interaction of ICMEs. In the category of "Sh+MC", the MC (also with a *Bs* field) following the sheath region was partly responsible for the development of the storm.

[23] In this paper, only the interplanetary structures that contributed to the storm main phase development are noted. Thus cases when combinations of structures lead to a more complex storm recovery phase are not considered as a cause of the geomagnetic storm itself. When there was a decrease of *Dst* followed by a recovery prior to the storm main phase development to $Dst \leq -100$ nT, this first structure was not considered.

3. Results

3.1. Examples of Interplanetary Drivers

[24] Examples of geomagnetic storms caused by each one of the 4 main interplanetary drivers are presented in

Table 1. Intense Magnetic Storms (Dst ≤ -100 nT) Used in This Study

Date	Dst_p (nT)	IP Structure
23/10/1996	−105	CIR
21/04/1997	−107	nsMC
15/05/1997	−115	SH/MC
11/10/1997	−130	SH/MC
07/11/1997	−110	SH
23/11/1997	−108	sMC
18/02/1998	−100	nonMC/HCS
10/03/1998	−116	CIR
04/05/1998	−205	SH
26/06/1998	−101	COMPLEX nonMC/kinky HCS
06/08/1998	−138	SH/HCS/WAVE
27/08/1998	−155	nonMC
25/09/1998	−207	SH
19/10/1998	−112	sMC
08/11/1998	−149	SCOMPRMC
09/11/1998	−142	sMC
13/11/1998	−131	SH/MC
13/01/1999	−112	nonMC
18/02/1999	−123	SH
22/09/1999	−173	sMC
22/10/1999	−237	nonMC/CIR
13/11/1999	−106	COMPLEX
12/02/2000	−133	SH/MC
07/04/2000	−288	SH
24/05/2000	−147	CIR
16/07/2000	−301	sMC
11/08/2000	−106	nonMC
12/08/2000	−235	SH/MC
17/09/2000	−201	MC
05/10/2000	−181	COMPLEX
14/10/2000	−107	sMC
29/10/2000	−127	sMC
06/11/2000	−159	SH/MC
29/11/2000	−119	nonMC
20/03/2001	−149	sMC
31/03/2001	−387	SH/MC
11/04/2001	−271	SH/MC
18/04/2001	−114	SH
22/04/2001	−102	sMC
17/08/2001	−105	SH
26/09/2001	−102	SH
01/10/2001	−148	nonMC
03/10/2001	−166	nsMC
21/10/2001	−187	SH
28/10/2001	−157	SH
06/11/2001	−292	SH
24/11/2001	−221	SH/MC
24/03/2002	−100	SH
18/04/2002	−127	SH/MC
20/04/2002	−149	SH/MC
11/05/2002	−110	SH
23/05/2002	−109	SH
02/08/2002	−102	SH
21/08/2002	−106	nsMC
04/09/2002	−109	CIR
08/09/2002	−181	SH/nonMC
01/10/2002	−176	sMC
04/10/2002	−146	sMC
07/10/2002	−115	CIR
14/10/2002	−100	CIR
21/11/2002	−128	CIR
29/05/2003	−144	SH
18/06/2003	−141	SH
12/07/2003	−105	CIR
18/08/2003	−148	sMC
30/10/2003	−353	SH/MC
30/10/2003	−383	SH
20/11/2003	−422	sMC
22/01/2004	−149	nonMC
11/02/2004	−109	CIR
04/04/2004	−112	SH
23/07/2004	−101	nonMC
25/07/2004	−148	sMC
27/07/2004	−197	SH/MC
30/08/2004	−126	sMC
08/11/2004	−373	sMC
10/11/2004	−289	SH/MC
12/11/2004	−109	SH
18/01/2005	−121	CIR
22/01/2005	−105	SH
08/05/2005	−127	CIR
15/05/2005	−263	sMC
20/05/2005	−103	nsMC
30/05/2005	−138	nonMC
13/06/2005	−106	sMC
24/08/2005	−216	sMC
31/08/2005	−131	CIR
11/09/2005	−123	SH
14/04/2006	−111	sMC
15/12/2006	−147	sMC

Figures 1 through 4: magnetic storms caused by sMC, Sh, Sh +MC and CIR, respectively. Figures 5 and 6 are examples of non-MC ICME and a ICME/kinky HCS, respectively. For each of these figures, the proton temperature, solar wind speed, proton density, magnetic field magnitude and components (GSM), plasma beta, solar wind dynamic pressure, dawn-dusk electric field and the *Dst* index are shown. The storm main phase is indicated by the solid bar in the bottom of panels. Each event will be discussed in detail below.

[25] Figure 1 shows a sMC driven storm during 29–31 August 2004. The MC interval is marked with the solid lines and by the arrow bar. The MC boundaries are defined by the drop in the plasma beta parameter and the rotation in *Bz* component. An interplanetary shock, indicated by a dotted vertical line, is observed at ∼09:00 on day 29 August. It was followed by a magnetospheric sudden impulse (not shown) at ∼10:00 UT. The ∼1-h difference is due to the solar wind propagation from ACE to Earth. An IMF *Bs* structure is noted on day 30, when ACE was in a low-beta region. The *Bz* shows a smooth rotation, indicating a MC. This *Bs* structure is the cause of the *Dst* decrease and of the storm main phase. The geomagnetic storm has a long and monotonic development before the peak *Dst*, which occurred at 22:00 UT on 30 August (*Dst* = −126 nT).

[26] Figure 2 shows a geomagnetic storm caused by sheath fields during 29–30 May 2003. An interplanetary shock is observed at ∼12:00 UT on day 29 (marked with a S1). This first shock and its sheath did not contributed to the storm main phase. A second shock is detected at ∼18:00 UT on day 29 and the IMF Bs in the sheath led to the storm main phase. The shock is indicated by a vertical dotted line and marked by S2. The sheath interval is the region between the shock (dotted line) and the solid line, marked with the arrow bar. The IMF components are highly fluctuating in the sheath region. There are weak *Bs* fields upstream of the second shock. Shock compression intensified the *Bs* component and the latter caused the magnetic storm (see *Tsurutani et al.* [1988] for discussions of shock compression). The storm development is complex with several Dst

Table 2. Interplanetary Structures That Caused Intense Geomagnetic Storms Per Year During Cycle 23

Year/IP Structure	CIR	sMC	Sh+MC	Sh	nsMC	nonMC	Sh+nonMC	nonMC+HCS	Sh+HCS	S.compr MC	nonMC+CIR	Complex	Total
1996	1	-	-	-	-	-	-	-	-	-	-	-	**1**
1997	-	1	2	1	1	-	-	-	-	-	-	-	**5**
1998	1	2	1	2	-	1	-	1	1	1		1	**11**
1999	-	1	-	1	-	1	-	-	-	-	1	1	**5**
2000	1	4	3	1	-	2	-	-	-	-	-	1	**12**
2001	-	2	3	6	1	1	-	-	-	-	-	-	**13**
2002	4	2	2	4	1	-	1	-	-	-	-	-	**14**
2003	1	2	1	3	-	-	-	-	-	-	-	-	**7**
2004	1	3	2	2	-	2	-	-	-	-	-	-	**10**
2005	3	3	-	2	1	1	-	-	-	-	-	-	**10**
2006	-	2	-	-	-	-	-	-	-	-	-	-	**2**
Total	**12**	**22**	**14**	**22**	**4**	**8**	**1**	**1**	**1**	**1**	**1**	**3**	**90**

CIR: corotating interaction region;
MC: ICME that shows the signature of a magnetic cloud;
sMCs: MC preceded by a fast shock;
nsMC: MC not preceeded by a fast shock;
Sh+MC: sheath field followed by a magnetic cloud;
Sh: sheath field;
nonMC: ICME that does not shows the signature of a magnetic cloud;
HCS: crossing of the heliospheric current sheet;
S compr MC: magnetic cloud compressed by shock.

decreases prior to the storm peak at 02:00 UT on 30 May, with minimum *Dst* of −131 nT.

[27] Figure 3 is an example of a geomagnetic storm caused by a combination of sheath and MC fields on 26–27 July 2004. Again, a dotted vertical line denotes the interplanetary shock. Solid vertical lines bound the MC, also marked with arrow bar. A shock is observed at ∼22:00 UT on day 26. There is an irregular *Bs* field feature in the sheath behind the shock causing a *Dst* decrease and the start of the storm. Shock compression of upstream southward *Bz* was the cause of the southward sheath fields. During day 27, a low beta region with a rotating *Bz* impinged upon the magnetosphere. The latter structure was a MC. The southward component of the MC led to the intensification of the storm main phase. A peak *Dst* of −197 nT was reached at 13:00 UT 27 July 2004.

[28] Figure 4 is an example of a geomagnetic storm caused by a CIR, which interval is marked by the bar in the magnetic field magnitude panel, during 21 November 2002. The high speed stream (HSS) and low speed stream (LSS) as well the region of compressed magnetic field and plasma (the CIR, indicated with arrow bar) are also indicated in the Figure. The storm began on day 21 November at 02:00 UT. It was caused by the southward components of oscillating *Bz* fields within the CIR. The storm peak occurred at 10:00 UT on 21 November, with a peak *Dst* of −128 nT. Note that there is ongoing activity at this time, but this is interrupted by the period of strong northward fields prior to the onset of the intense storm.

[29] Figure 5 is an example of a magnetic storm caused by a nonMC ICME, during 10–12 August 2000. This ICME does not have a clear NS or SN *Bz* rotation as required by *Burlaga et al.* [1981]. The interplanetary shock (∼04:00 UT 10 August) is indicated and the ICME interval (∼1900 10 August to ∼1900 11 August) denoted by solid vertical lines. There is a long interval of IMF *Bs* fields, around ∼10 nT, that led to the storm main phase. This *Bs* interval persisted for almost one day. No clear rotation in the magnetic field components is noted. We note that this is not a MC according to our criteria because it does not shows a full *By* or Bz rotation (from positive to negative values or vice versa), but it has been considered as a MC by other authors due to the smooth change in *Bz* component [e.g., *Huttunen et al.*, 2005].

[30] Figure 6 shows an example of a magnetic storm caused by combination of a kinky HCS and ICME/nonMC fields. The storm main phase is observed during 26 June 1998. The IMF *Bs* cause of the storm is the sharp southward turning of the IMF *Bz* component at the end of day 25 and start of day 26. There is a shock prior to the arrival of the *Bz* southward interval. The shock is noted by a jump in plasma parameters and in *B* (indicated by dotted lines in this figure). This shock is preceded by a MC ICME and followed by a nonMC ICME, according to the *Cane and Richardson* [2003] catalogue. Their boundaries are marked with solid lines. However, after the shock, we notice a large solar wind density value, which could still be just sheath material. Upstream of the shock, there is a high speed solar wind period starting on day 24, not preceded by a shock. This might have occurred because of the high density upstream of the stream caused the damping of the shock. After the arrival of this high speed stream, there is a region of low *Tp* and beta, intense *B* and a rotating *Bz.* This region corresponds to the MC reported by *Cane and Richardson* [2003], which ended at the shock arrival. The IMF polarity changes during this event. From the *Bx* and *By* components, we note that the HCS is crossed in the end of day 23, then it is crossed again by the end of day 25, and a final HCS crossing is detected at beginning of day 26. A high density region upstream of MC is seen on days 23–24 and a reversal in *Bx* and *By* polarities on day 23. This is interpreted as a signature of a HCS crossing. The high density might be the plasma sheet of the HCS.

[31] The interpretation that the MC ended at the shock is not the only possibility. There are discontinuities in *By* and a low beta region that could indicate the true end of the MC (marked with the second solid line in the Figure 6). Thus we have two possible interpretations for the origin of this

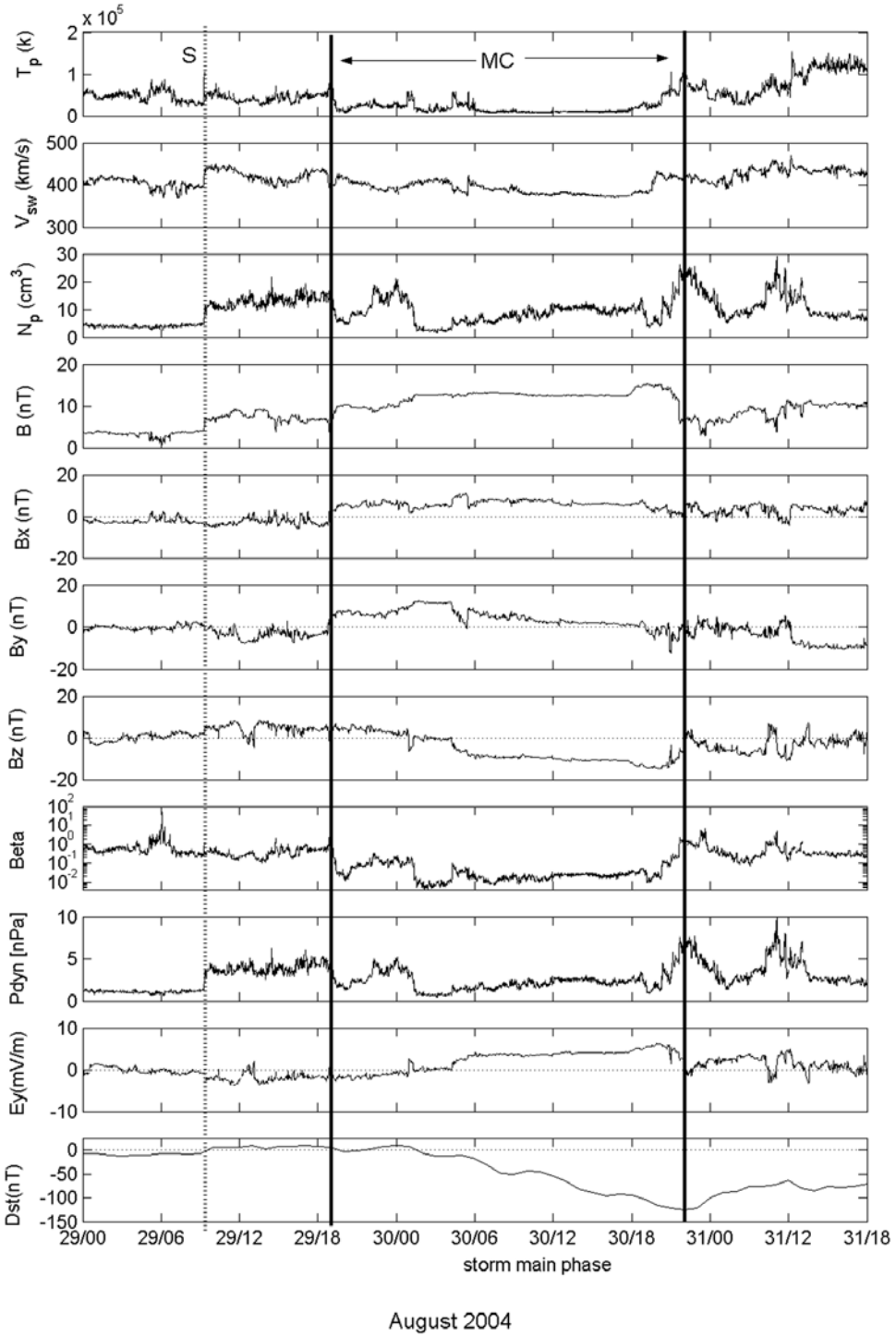

Figure 1. Example of an intense magnetic storm caused by a magnetic cloud; 29–31 August 2004.

storm: (1) the first interpretation is that the initial part of the IMF *Bs* leading to the storm is shocked MC. For this interpretation, the MC ends where the beta/*By* discontinuity are marked. The second part of the *Bs* is either sheath of MC fields; (2) the second interpretation is that the second stream (second peak in Vsw) has strongly deflected the IMF fields. The *Bx* and *By* fields reverse direction at the shock. The *By* discontinuity is the HCS and the field *By* and *Bx* polarities reverse direction there. So in this case the *Bs* is caused by the shock compression and deflection of the HCS. A case of a kinky HCS causing geomagnetic activity has been reported previously [*Tsurutani et al.*, 1984]. However, this may be the first example of a HCS causing an intense storm case.

3.2. Statistics of All Storms and Relation With Interplanetary Parameters

[32] Figure 7 shows the solar cycle distribution of intense storms. For this solar cycle (23), there is a three peak distribution, 1998, 2001–2002 and 2004–2005. The peaks

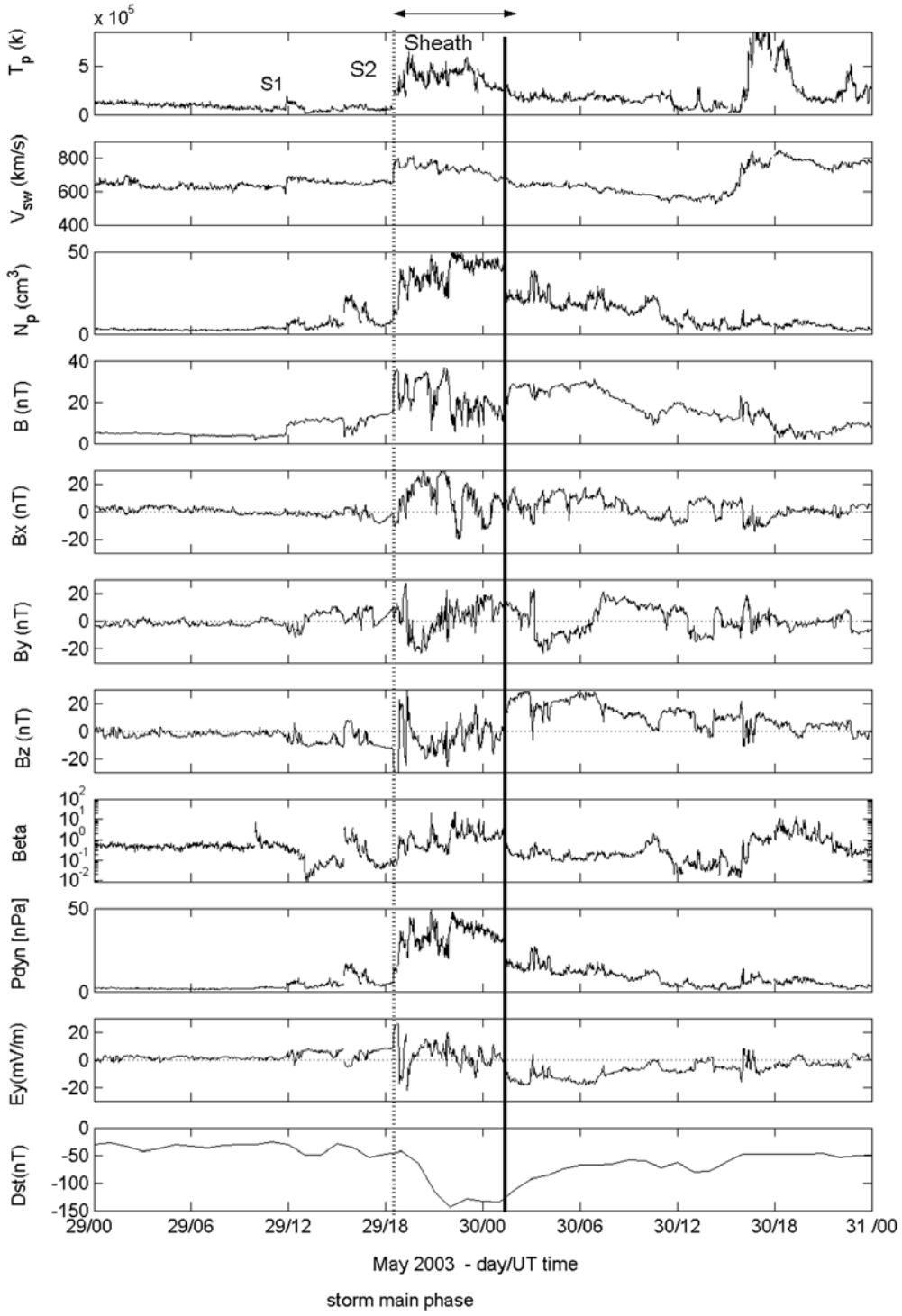

Figure 2. Example of an intense magnetic storm caused by sheath fields; 29–31 May 2003.

at 2001–2002 and 2004–2005 correspond to the solar maximum and declining phase peaks, which *Gonzalez et al.* [1990] have reported for several solar cycles. The presence of the extra peak in the rising phase is somewhat unexpected. Notice, however, that this peak occurs only in 1998, which might be an atypical year compared to other rising phase years. On the other hand, another possibility is that 1999 could be an unusual year, with a low rate of intense magnetic storms. These distributions should be studied with more detailed interplanetary and solar observations.

[33] Figure 8 shows the histograms for integrated *Bs* and *Ey*, and peak *Dst*, *Bs* and *Ey* for all of the intense storms. The distributions for *Dst* and *Bs* are shown for $-Dst$ and $-Bs$ to help to compare their histograms with the other parameters. Peak values are determined during the storm main phases, prior to peak *Dst* values. Integrated values are also taken along the main phases, but only negative *Bz* and

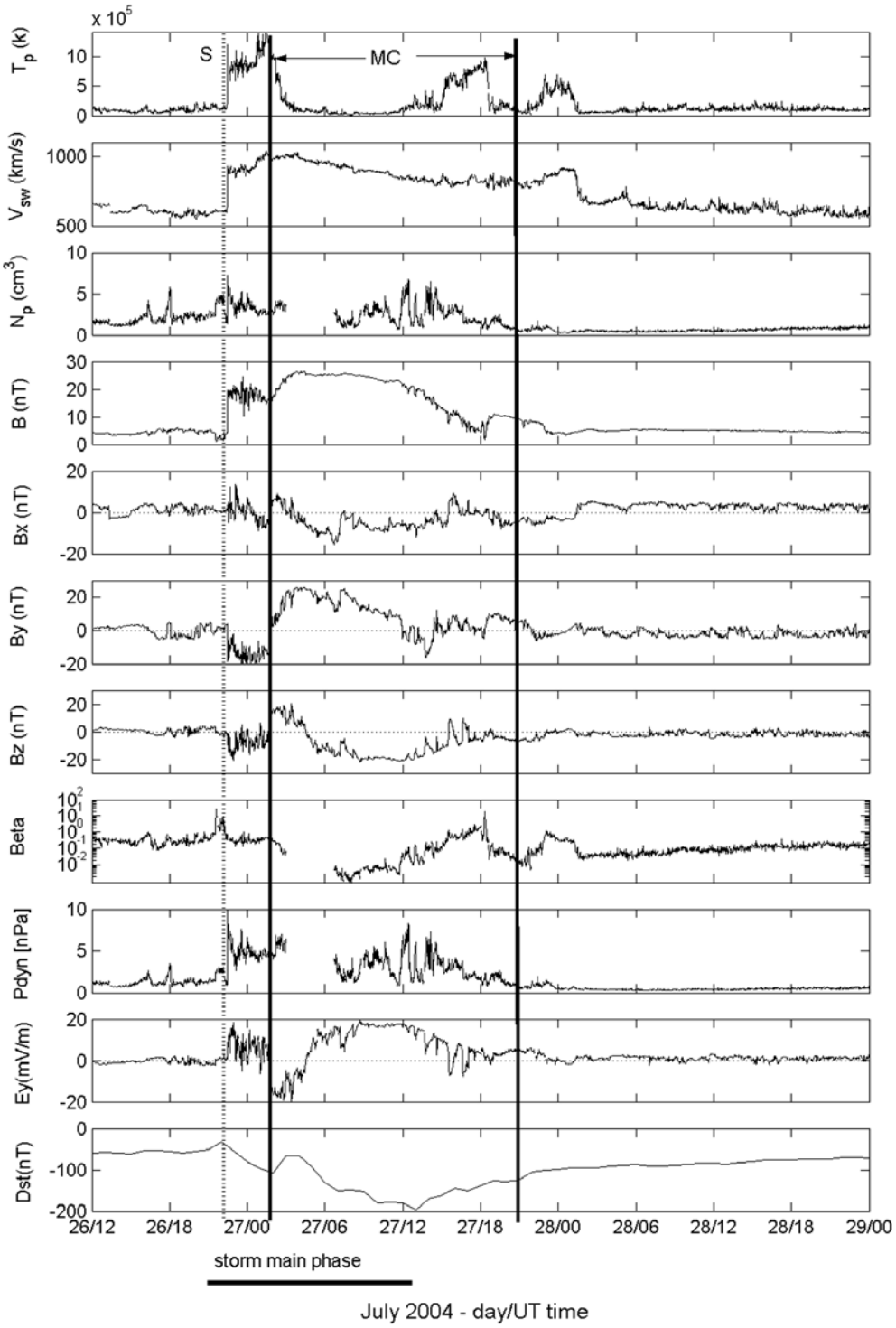

Figure 3. Example of an intense magnetic storm caused by MC+Sheath fields; 26–29 July 2004.

positive *Ey* are taken into account. Most storms (~2/3) have peak *Bs* between 10–20 nT, and peak *Ey* between 5–10 mVm^{-1}. Integrated values of *Bs* are for most of cases lower than 200 nT.h and for *Ey* lower than 100 mV.m^{-1}.h. The *Dst* distribution shows a larger number of storms around −100 to −150 nT.

[34] We investigate next the dependence of peak *Dst* on interplanetary parameters. Figure 9 shows the correlation of peak *Dst* with peak values of *Bs*, *Ey*, positive and negative *By* values, total magnetic field *Bp*, dynamic pressure *Pdyn*, density *Np* and velocity *Vsw*. The interplanetary peak values were taken along the storm main phase. We can see that the highest correlation values are found with *Bs* and *Ey*. This indicates a higher dependence of *Dst* with the *Bs* or *Ey* parameters. The high correlation with *Bp* (r = 0.78) occurs because when *Bs* is high usually the total field is also high

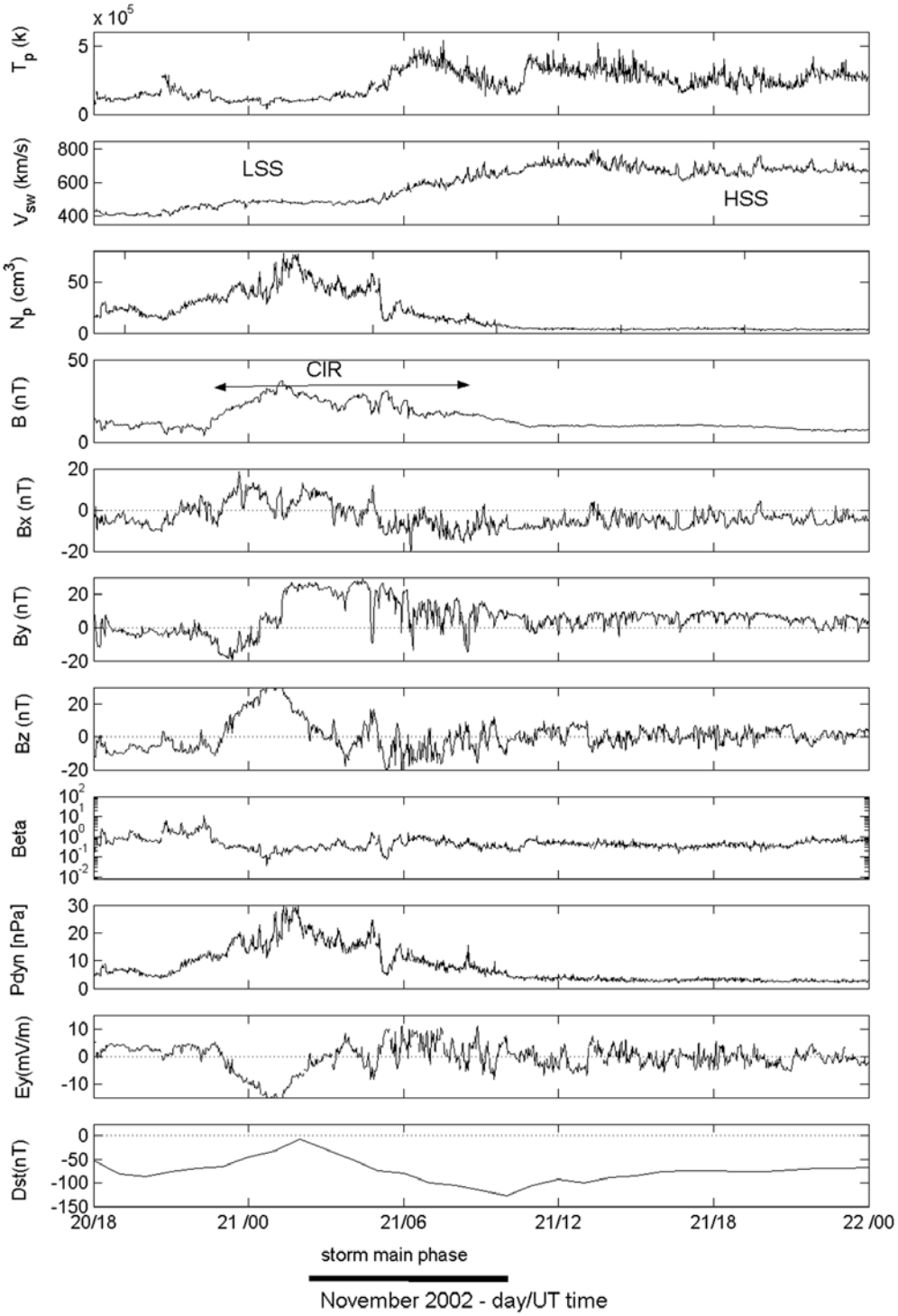

Figure 4. Example of an intense magnetic storm caused by corotating streams; 20.75–22 November 2002.

(the correlation coefficient between *B*s and *Bp* is r = 0.8). The same could occur with the correlations with *By* components, because *Bz* and *By* can increase together. The correlation with integrated *Bs* and *Ey* is 0.42 and 0.68, respectively, values much lower than with peak *Bs* and *Ey*.

[35] We further assess the *Dst* dependence on interplanetary parameters by calculating linear multiregressions. We ran a multilinear regression model for three situations, with *Dst* as a function of 1) *Bz* and *By*−, 2) *Bz* and *By*+; and 3) *Bz* and *Pdyn*. This model is of the form $Dst = a0 + a_{Bz}Bz + a_{By}By - (a_{By}By \text{ or } a_{Pdyn}Pdyn)$.

[36] The model gives the multilinear correlation coefficients, the coefficients of the dependent variables and their standard deviations.

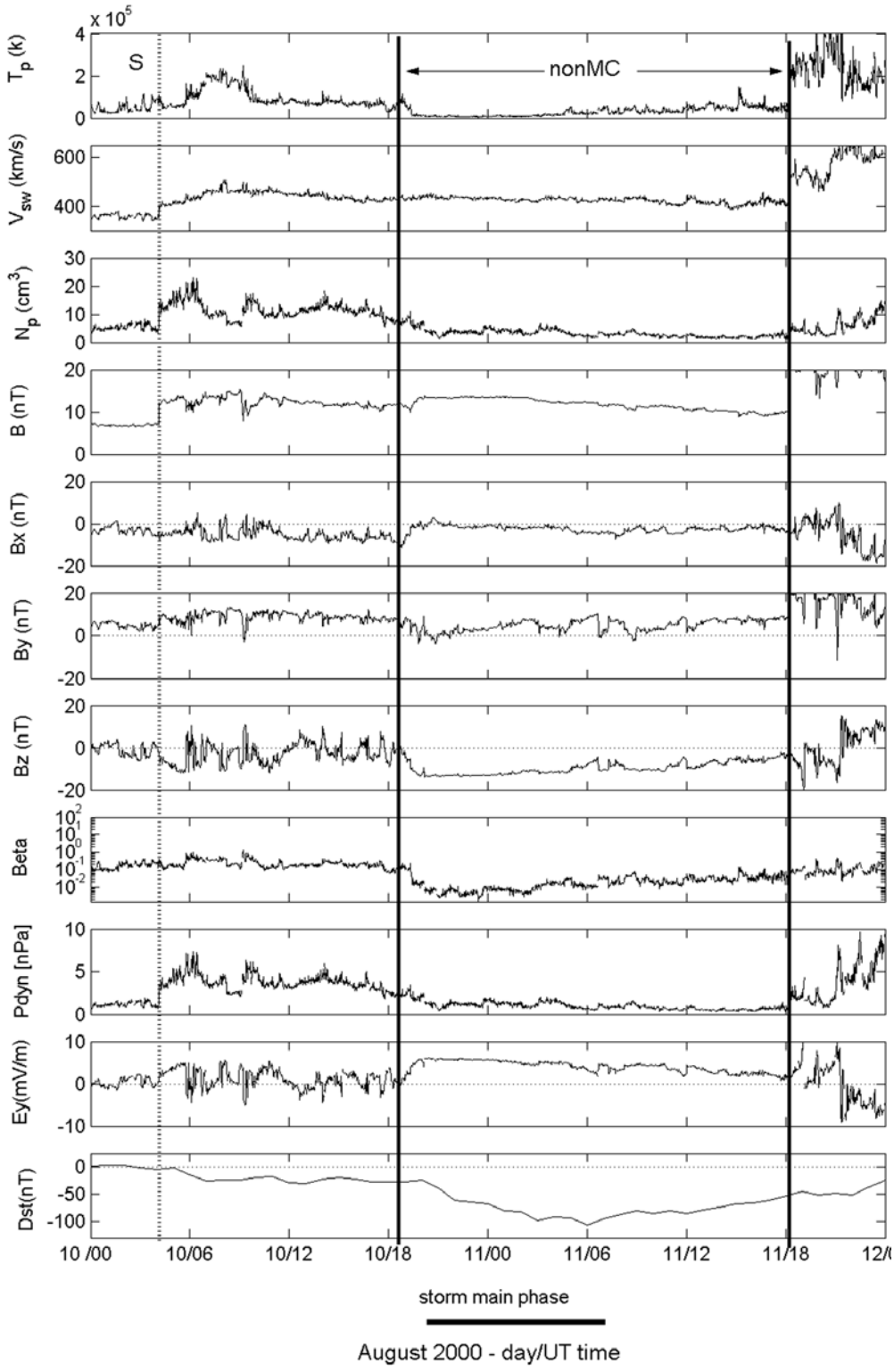

Figure 5. Example of an intense magnetic storm caused by ICME (non-MC) 10–12 August 2000.

[37] The correlation coefficients are, respectively, r^2 = 0.63, 0.64, 0.75. The regression coefficients are:

1) Bz and By− : $a_{Bz} = 5.5 \pm 0.75$; $a_{By-} = 0.78 \pm 0.98$;
2) Bz and By+ : $a_{Bz} = 5.5 \pm 0.73$; $a_{By+} = -0.38 \pm 0.84$;
3) Bz and Pdyn : $a_{Bz} = 5.7 \pm 0.45$; $a_{Pdyn} = -0.82 \pm 0.38$.

[38] We note that the coefficients for *Bz* dependence are much higher than for *By*. The *Bz* coefficients are also much higher than their errors, which is not the case for *By* and *Pdyn*. Thus we may conclude that peak *Dst* shows a much higher dependence on *Bs* than on *By* or *Pdyn*, which

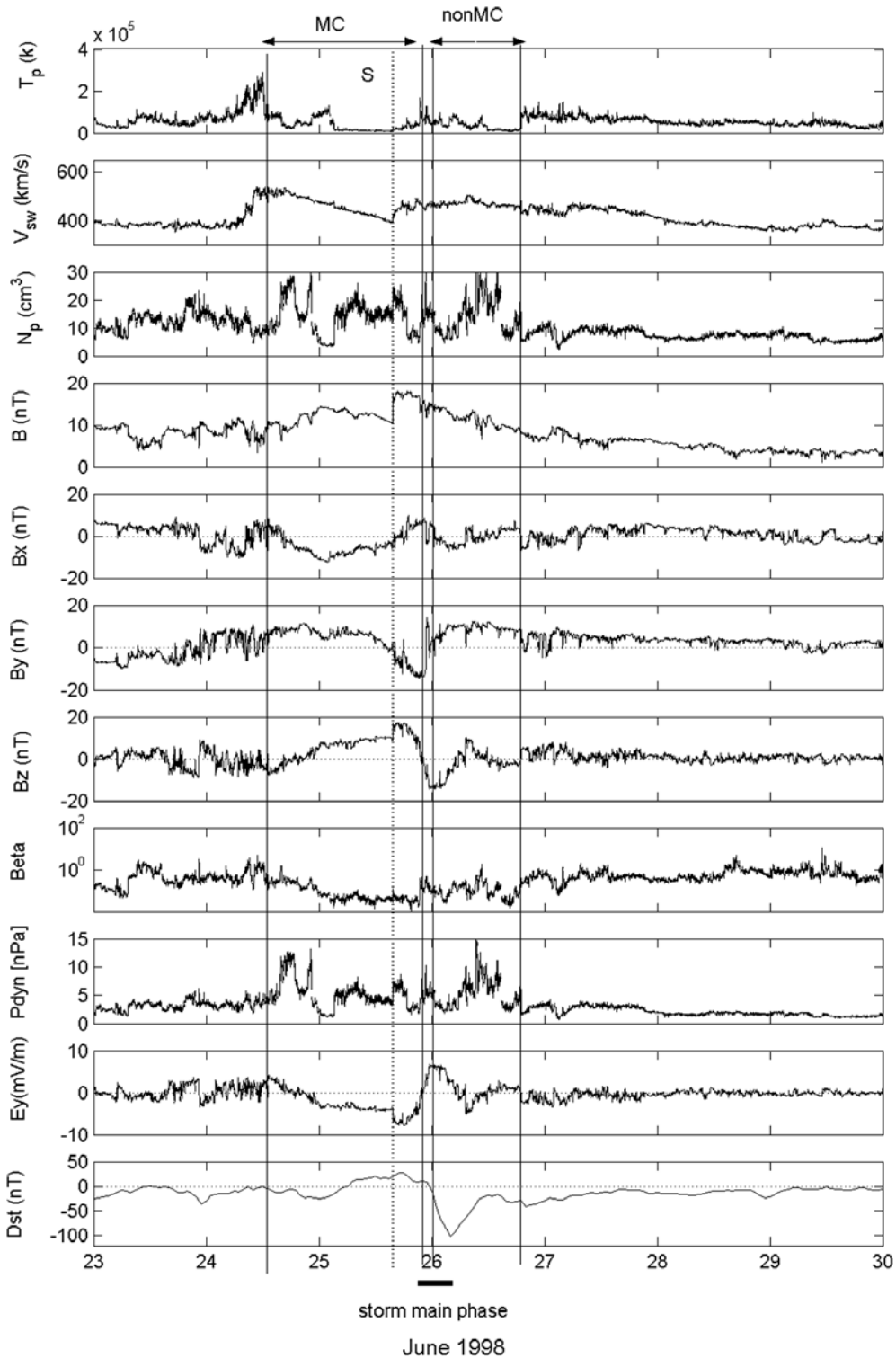

Figure 6. Example of an intense magnetic storm caused by a kinky HCS/ICME; 23–29 June 1998.

constitutes evidence for the magnetic reconnection mechanism causing storms.

3.3. Ey Criteria

[39] We have tested the *Gonzalez and Tsurutani* [1987] - GT interplanetary *Ey* criteria for all the intense storms. This empirical criteria states that a necessary interplanetary condition for an intense geomagnetic storm occur is the presence of an intense ($Bs > 10$ nT or $Ey > 5$ mV/m) for long durations ($t > 3$ h) of time. We have also tested other slightly different Ey criteria. The results are summarized in Table 3.

[40] We have found that 68% of the storms meet the GT criteria. From the IP driving classes (Table 1) we have found that 17% of CIR, 77% of sMC, 78% of Sh+MC and 73% of

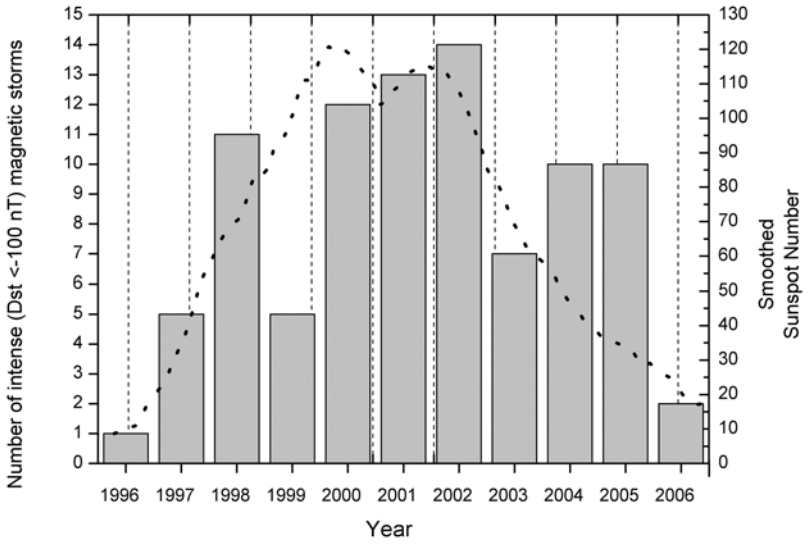

Figure 7. Yearly count of intense storms during solar cycle 23 (1996–2006).

Sh storms satisfy the criteria. Thus CIR storms are a class of storms that usually do not satisfy the GT criteria, probably because of the highly fluctuating fields. From the other IP driving structure class, 75% of the storms satisfy the GT criteria. We have found more general criteria, satisfied by ~90% of the storms, is $Ey \geq 3$ mV/m for a time longer than 3 h.

[41] We have further tested the GT criteria according to the storm intensity. We have classified storms in two classes, those with $Dst > -150$ nT (62 storms) and others with $Dst \leq -150$ nT (28 storms). We have found that 50% of the storms with $Dst > -150$ nT satisfy the GT criteria, while ~93% of the stronger storms meet the GT criteria. The GT *Ey* criteria are thus satisfied for the more intense storms but not for some of the weaker storms. *Echer et al.* [2008] have also found that all the superstorms ($Dst \leq -250$ nT) during cycle 23 satisfied the GT criteria (as expected).

3.4. Solar Cycle Dependence

[42] From Table 2, it is found that the four most common interplanetary structures responsible for intense storm development are Sh, sMC, Sh+MC and CIR fields. Figure 10 show two pie chart diagrams with the interplanetary drivers of intense storms during cycle 23. In Figure 10a, we show the four main causes: sMC (24.4%), Sh (24.4%), Sh+MC (15.5%) and CIR (13.3%). These four interplanetary drivers contribute, to ~77% of the intense storms in cycle 23, or ~3/4 of the total. Next we group together all the ICME types: sMCs, nsMC and nonMC, and present the results in Figure 10b, with the general label of ICME and Sh+ICME. We can see that 37.8% are caused by the ICME fields. The number of storms that are not caused by ICME, Sh, Sh+ICME or CIR is only 7.8%. These cases correspond to several special storms (Tables 1 and 2), caused by interaction of ICME and CIR, ICME-ICME interaction (complex causes), MC-shock interaction, shocked HCS (Table 3).

[43] There were 11 superstorms ($Dst \leq -250$ nT) during cycle 23. About 1/3 of the superstorms were caused by magnetic clouds (MCs), 1/3 by a combination of sheath and MC fields, and 1/3 by sheath fields alone. For more details see *Echer et al.* [2008].

[44] The annual distribution of the four main interplanetary causes is represented with the point symbols in Figure 11a. The open squares represent CIR, solid circles Sh+MC, stars sMC fields and open triangles Sh fields. We have classified

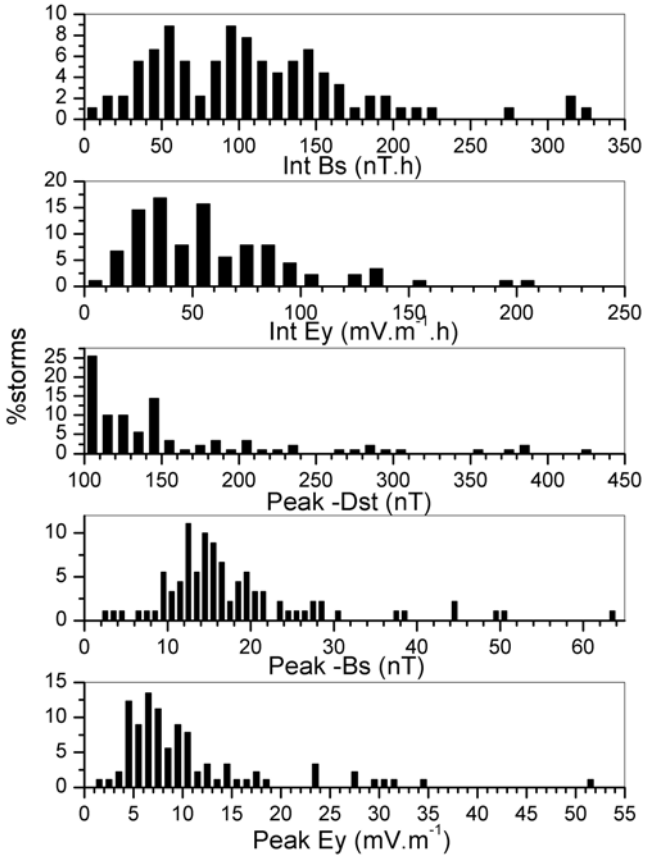

Figure 8. Histograms of integral values of Bs and Ey, and peak values of Dst, Bs, and Ey for all the magnetic storms.

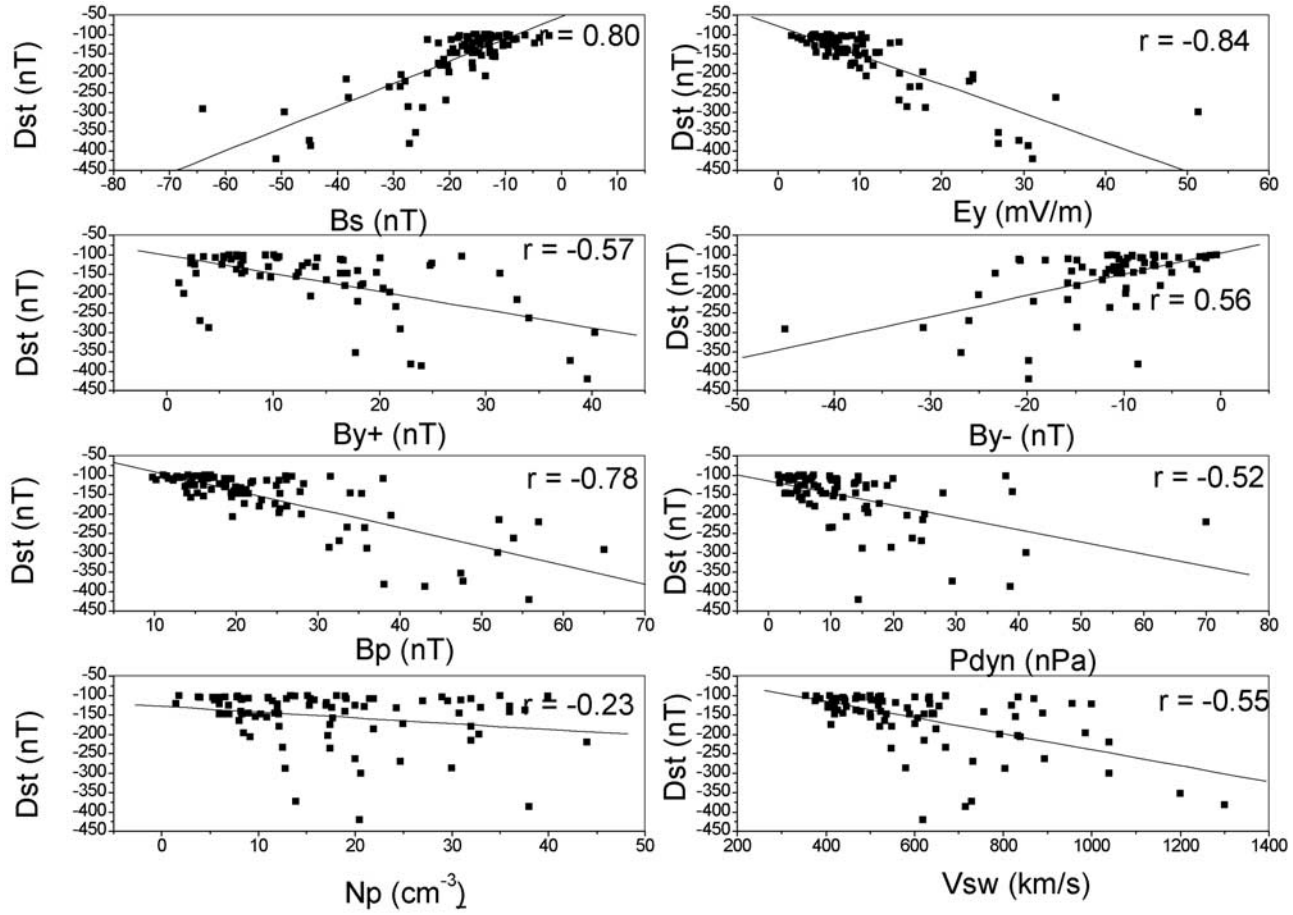

Figure 9. Correlation between peak Dst and interplanetary parameters: peak Bs, Ey, By+, By−, Bp, Pdyn, Np, and Vsw.

the solar cycle, based on the sunspot curve asymmetry, in minimum/rising phase (1996–1998), maximum (1999–2002) and declining/minimum phase (2003–2006). This classification took into account the fact that rising phases are shorter than declining phases [*Lang*, 2001]. The results are shown in Figure 11b. We have found more storms in the maximum and declining phases than in the rising phase. During the rising phase, Sh+MC and sMC are the interplanetary structures that led to more storms. At solar maximum, Sh fields are responsible by a larger number of storms, followed by sMC fields. In the declining phase, there is a predominance sMC producing storms, followed by Sh and CIR fields. Note that these results are different from *Gonzalez et al.* [2007], because of the different criteria used to divide the solar cycle into parts. Here CIR events are divided in solar maximum and declining phases, but most of CIRs occurred in 2002. Some general features are observed from both studies:

Table 3. Interplanetary Criteria for the Intense Geomagnetic Storms of Cycle 23

IP Criteria	N. Storms That Meet the Criteria	% Storms That Meet the Criteria
Ey $\geq$ 2 mV/m; t $\geq$ 3 h	84	93%
Ey $\geq$ 3 mV/m; t $\geq$ 3 h	79	88%
Ey $\geq$ 5 mV/m; t $\geq$ 2 h	72	80%
Ey $\geq$ 5 mV/m; t $\geq$ 3 h (GT87)	61	68%

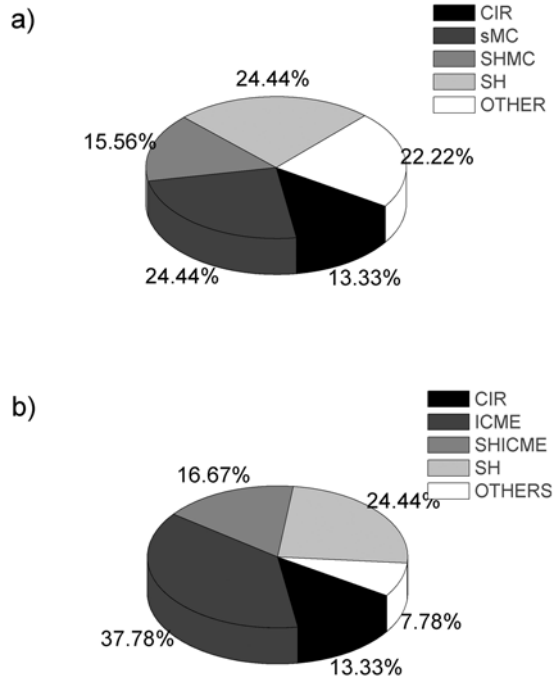

Figure 10. Pie chart diagrams showing the interplanetary causes of intense geomagnetic storms during cycle 23.

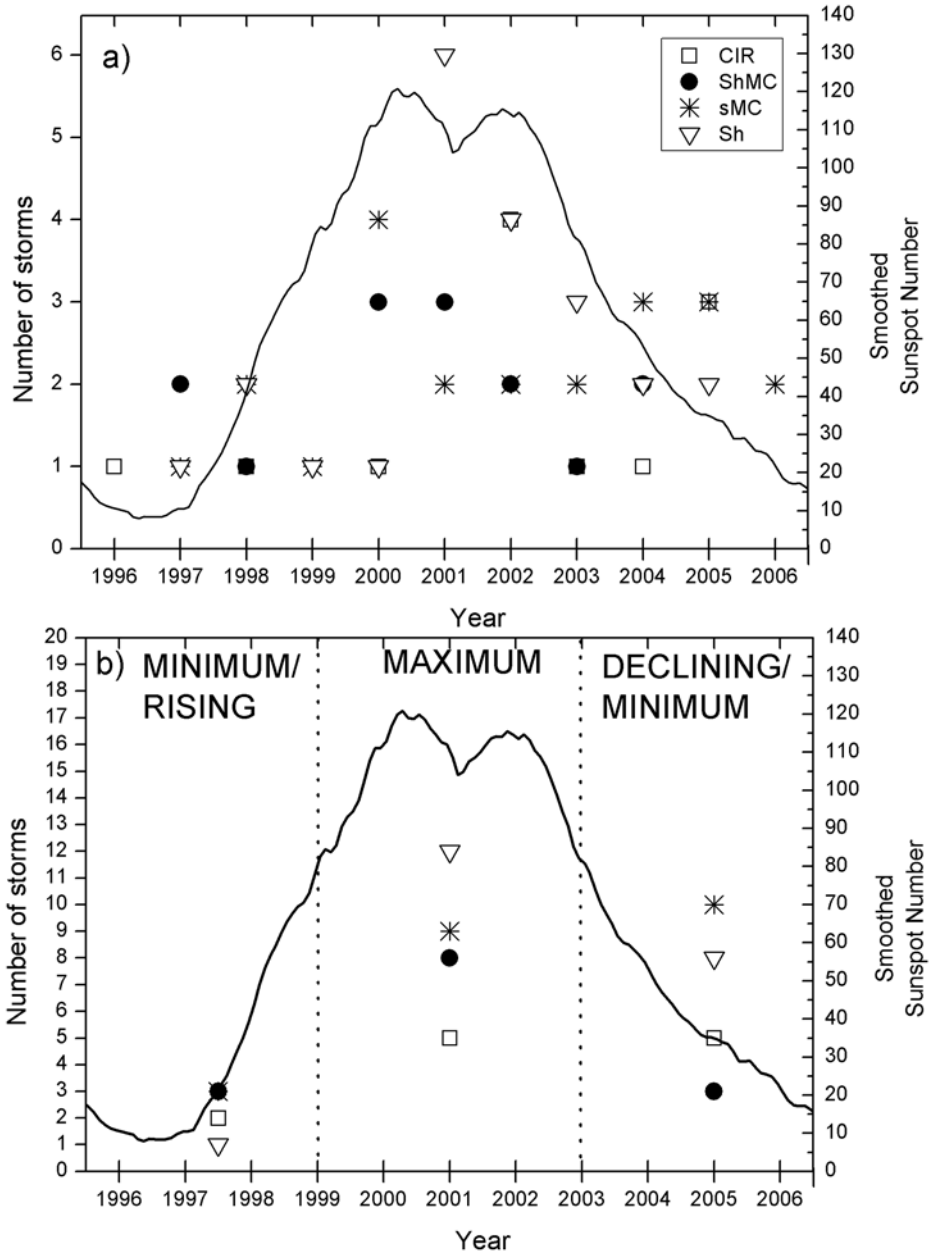

Figure 11. Distribution of storms driven by the four main interplanetary structures per year (a) and per solar cycle phase (b).

there is greater importance of sheath fields in the solar maximum phase; sMC fields causes more storms than sheath field during the rising and declining phases; the CIR fields are more important in causing storms in the late solar maximum phase/post-maximum phase and in the declining phase.

4. Summary and Discussions

[45] We have studied the interplanetary causes and conditions that lead to intense geomagnetic storms during solar cycle 23 (1996–2006). We have found that all 90 of the storms studied in this paper were caused by IMF *Bs* fields. We have not found any contrary event. Both linear correlation and multiple linear correlation showed much higher dependence of *Dst* on *Bs*/*Ey* than on any other interplanetary parameter. These results indicate that the possibility that intense storms of Dst ≤ -100 nT intensity may be caused by intense solar wind pressure (shocks), high speed streams, IMF *By* and *Bz* north conditions is slight or nonexistent. Magnetic reconnection due to intense southward IMFs is the dominant mechanism. Although this study puts a limit on the possible magnetospheric energy input role of viscous interaction mechanisms, one can not rule out the possibility that viscous interaction makes a substantial contribution in intensifying magnetic storms caused by magnetic reconnection. Further studies are obviously necessary.

[46] We have tested empirical interplanetary criteria of long duration (>3 h) $Bs \sim 10$ nT or $Ey \sim 5$ mV. m^{-1} leading to intense storms [*Gonzalez and Tsurutani*, 1987]. We have found that ~70% of the storms studied in this work satisfied

these criteria. Of the storms that did not follow the GT *Ey* criteria, the main types of structures are CIRs (only 17% meet the GT criteria). We have found that a more general *Ey* criteria (followed by ~90% of the storms) is $Ey \geq 3$ mV/m for a time longer than 3 h.

[47] The ranges of peak *Dst* values for the 4 main IP drivers are: CIR [−100 to −147 nT], sMC [−103 to −472 nT], Sh [−101 to −288 nT], and Sh+MC [−115 to −289 nT]. Note that the lower limit is artificial, because of the criterion of Dst < −100 nT for selection of the storms. The upper limit of CIR generated storms is below the upper limits of other structures. The biggest events are generated by MCs.

[48] The interplanetary structures leading to the intense storms have been identified. It was found that the main structures responsible by driving storms are sMC (24.4%), Sh (24.4%), ShMC (15.5%), and CIR (13.3%). These four driving classes are responsible for almost three-fourths of intense storms during cycle 23. When all ICMEs are considered, we found that more than 90% of intense storms are caused by ICME and/or their sheath fields, and CIR fields.

[49] The most important storm drivers, according to the solar cycle phases, are:

[50] - Minimum/Rising phase: sMC and sheath fields;

[51] - Solar Maximum: sheaths, and sheath+MC fields.

[52] - Declining/minimum phase: sMC, sheaths and CIRs.

[53] The approximate rate of storms per solar cycle phase is: min/rising phase: 3 storms.year^{-1}; maximum phase: 8.5 storms.year^{-1}; declining/minimum phase: 6.5 storms.year^{-1}.

[54] From the results given in Figure 11, ICMEs (non-MC + sMCs + nsMC) are dominant in the rising/declining solar phases, while at solar maximum, sheath fields cause a larger number of storms. This higher occurrence of storms driven by sheath fields during solar maximum could imply that the presence of stronger and faster CMEs around this phase of the solar cycle. Faster ICMEs will result in stronger interplanetary shocks, which in turn will cause stronger sheath fields. Another possible explanation is that interplanetary conditions during solar maximum are more favorable to shock formation and propagation. This could happen due to the solar cycle variation of solar wind parameters near Earth's orbit [*Gorney*, 1990]. This hypothesis will be examined in a future work which will study the evolution/relationship of shock Mach number with solar cycle phase. CIRs are more important in the post maximum (2002) and declining phase due to the presence of large coronal holes extending equatorward and persisting for several solar rotations [*Tsurutani et al.*, 1995].

[55] **Acknowledgments.** Part of this work was done with the support of "Fundo de Desenvolvimento Cientifico e Tecnologico" of Brazil. We would like to thank to the Solar Physics Interactive Data Resources Center of NOAA for the Dst index and to the ACE and WIND teams for the solar wind data. EE would like to thank to the Brazilian FAPESP (2007/04492-4) and CNPq (PQ-300104/2005-7 and 470706/2006-6) agencies for financial supports. We also thank the ACE and WIND plasma and magnetometer teams for solar wind data. The BTT portion of this work was done at the Jet Propulsion Laboratory, Calif. Inst. Tech. under contract with NASA.

[56] Wolfgang Baumjohann thanks Ian Richardson and another reviewer for their assistance in evaluating this paper.

References

Axford, W. I., and C. O. Hines (1961), A unifying theory of high-latitude geophysical phenomena and geomagnetic storms, *Can. J. Phys*, *39*, 1433.

Balogh, A., et al. (1999), Corotating interaction regions, *Space Sci. Rev.*, *89*, 141.

Burlaga, L. F., and S. Ogilvie (1970), Magnetic and thermal pressures in the solar wind, *Sol. Phys.*, *15*, 61.

Burlaga, L. F., et al. (1981), Magnetic loop behind an interplanetary shock: Voyager, Helios and IMP-8 observations, *J. Geophys. Res.*, *86*(A8), 6673–6684.

Burlaga, L. F. (1995), *Interplanetary Magnetohydrodynamics*, Oxford Univ. Press, New York.

Burlaga, L. F., et al. (1998), A magnetic cloud containing prominence material: January 1997, *J. Geophys. Res.*, *103*(A1), 277–286.

Burlaga, L. F. (2001), Terminology for ejecta in the solar wind, *Eos Trans. AGU*, *82*(39), 433, doi:10.1029/01EO00265.

Cane, H. V., and I. G. Richardson (2003), Interplanetary coronal mass ejections in the near-Earth solar wind during 1996–2002, *J. Geophys. Res.*, *108*(A4), 1156, doi:10.1029/2002JA009817.

Daglis, I. A., et al. (1999), The terrestrial ring current: Origin, formation and decay, *Rev. Geophys.*, *37*(4), 407–438.

Dungey, J. W. (1961), Interplanetary magnetic field and the auroral zones, *Phys. Rev. Lett.*, *6*, 47–48.

Echer, et al. (2008), Interplanetary conditions leading to superintense geomagnetic storms (Dst < −250) during solar cycle 23, *Geophys. Res. Lett.*, *35*, L06S03, doi:10.1029/2007GL031755.

Fairfield, D. H., et al. (2003), Motion of the dusk flank boundary caused by solar wind pressure changes and the Kelvin-Helmholtz instability: 10–11 January 1997, *J. Geophys. Res.*, *108*(A12), 1460, doi:10.1029/2003JA010134.

Farrugia, C. J., L. F. Buralga, and R. P. Lepping (1997), Magnetic clouds and the quite-storm effect at earth, in *Magnetic Storms*, *Geophys. Monogr. Ser.*, vol. 98, edited by B. T. Tsurutani et al., p. 91, AGU, Washington, D.C.

Garrett, H. B. (1974), The role of fluctuations in the interplanetary magnetic field in determining the magnitude of substorm activity, *Planet. Space Sci.*, *22*, 111–119.

Gorney, D. J. (1990), Solar cycle effects on the near-Earth space environment, *Rev. Geophys.*, *28*(3), 315–336.

Gonzalez, W. D., and B. T. Tsurutani (1987), Criteria of interplanetary parameters causing intense magnetic storms (Dst < −100 nT), *Planet. Space Sci.*, *35*, 1101.

Gonzalez, W. D., A. L. C. Gonzalez, and B. T. Tsurutani (1990), Dual-peak solar cycle distribution of intense geomagnetic storms, *Planet. Space Sci.*, *38*, 181.

Gonzalez, W. D., et al. (1999), What is a geomagnetic storm?, *J. Geophys. Res.*, *99*, 5771–5792.

Gonzalez, W. D., B. T. Tsurutani, and A. L. Clua de Gonzalez (1999), Interplanetary origin of magnetic storms, *Space Sci. Rev.*, *88*, 529–562.

Gonzalez, W. D., et al. (2007), Interplanetary origin of intense geomagnetic storms (Dst < −100 nT) during solar cycle 23, *Geophys. Res. Lett.*, *34*, L06101, doi:10.1029/2006GL028879.

Gosling, J. T. (1997), Coronal mass ejections: An overview, coronal mass ejections, *Geophys. Monogr.*, *99*, 9–16.

Hudson, M. K., S. R. Elkington, J. G. Lyon, V. A. Marchenko, I. Roth, M. Temerin, J. B. Blake, M. S. Gussenhoven, and J. R. Wygant (1997), Simulations of proton radiation belt formation during storm sudden commencements, *J. Geophys. Res.*, *102*, 12087, doi:10.1029/96JA03995.

Hughes, W. J. (1995), The magnetopause, magnetotail and magnetic reconnection, in *Introduction to Space Physics*, edited by M. G. Kivelson and C. T. Russell, Cambridge Univ. Press, Cambridge, UK.

Hundhausen, A. J. (Ed.) (1972), *Coronal Expansion and Solar Wind*, Springer-Verlag, Berlin.

Hundhausen, A. J., et al. (1984), The morphology and geometry of coronal mass ejections, *Eos Trans. AGU*, *65*, 1069.

Huttunen, K. E. J., et al. (2005), Properties and geoeffectiveness of magnetic clouds in the rising, maximum and early declining phases of solar cycle, *Ann. Geophys.*, *23*, 625–641.

Kennel, C. F., et al. (1985), A quarter century of collisionless shock research, in *Collisionless Shocks in the Heliosphere: A Tutorial Review*, edited by R. G. Stone and B. T. Tsurutani, *AGU Geophys. Monogr. Ser.*, vol. 34, pp. 1–36, AGU, Washington, D. C.

Lang, K. (2001), *The Cambridge Encyclopedia of the Sun*, Cambridge Univ. Press, Cambridge, UK.

Russell, C. T. (2001), In defense of the term ICME, *Eos Trans. AGU*, *82*(39), 434, doi:10.1029/01EO00266.

Schatten, K. H., and J. M. Wilcox (1967), Response of geomagnetic activity index Kp to interplanetary magnetic field, *J. Geophys. Res.*, *72*(21), 5185–5191.

Schwenn, R. (1996), An essay on terminology, myths, - and known facts: Solar transient-flares-CME-driver gas-piston-BDE-magnetic cloud-shock wave-geomagnetic storm, *Astrophys. Space Sci.*, *243*, 187–193.

Schwenn, R. (2006), Space weather: The solar perspective, *Living Rev. Sol. Phys.*, *3*, 1–76.

Smith, E., and J. H. Wolfe (1976), Observations of interaction regions and corotating shocks between one and 5 Au - Pioneer-10 and Pioneer-11, *Geophys. Res. Lett.*, *3*(3), 137–140.

Smith, M. F., and M. Lockwood (1996), Earth's magnetospheric cusp, *Rev. Geophys.*, *34*(2), 233–260.

Tsurutani, B. T., and R. M. Thorne (1982), Diffusion processes in the magnetopause boundary layer, *Geophys. Res. Lett.*, *9*(11), 1247–1250.

Tsurutani, B. T., and W. G. Gonzalez (1995), The efficiency of viscous interaction between the solar wind and the magnetosphere during intense northward IMF events, *Geophys. Res. Lett.*, *22*(6), 663–666.

Tsurutani, B. T., and W. G. Gonzalez (1997), The interplanetary causes of magnetic storms: a review, *AGU Geophys. Monogr. 98, Magn. Storms*, 77–87.

Tsurutani, B. T., C. T. Russell, J. H. King, R. D. Zwickl, and R. P. Lin (1984), A kinky heliospheric current sheet: Cause of CDAW-6 substorms, *Geophys. Res. Lett.*, *11*(4), 339–342.

Tsurutani, B. T., et al. (1988), Origin of interplanetary southward magnetic fields responsible for major magnetic storms near solar maximum (1978–1979), *J. Geophys. Res.*, *93*(A8), 8519–8531.

Tsurutani, B. T., et al. (1992), Great magnetic storms, *Geophys. Res. Lett.*, *19*(1), 73–76.

Tsurutani, B. T., et al. (1995), Interplanetary origin of geomagnetic activity in the declining phase of the solar cycle, *J. Geophys. Res.*, *100*(A11), 21,717–21,733.

Tsurutani, B. T., et al. (1997), Preface, *AGU Geophys. Monogr. 98, Magn. Storms*, ix–x.

Tsurutani, B. T., et al. (1998), The January 10, 1997, auroral hot spot, horseshoe aurora and first substorm: ACME loop?, *Geophys. Res. Lett.*, *25*(15), 3047–3050.

Zhang, J., et al. (2007), Solar and interplanetary sources of major geomagnetic storms (Dst ≤ -100 nT) during 1996–2005, *J. Geophys. Res.*, *112*, A10102, doi:10.1029/2007JA012321.

E. Echer, A. L. C. Gonzalez, and W. D. Gonzalez, Instituto Nacional de Pesquisas Espaciais (INPE) – POB 515, Sao Jose dos Campos, Sao Paulo 12227-010, Brazil. (eecher@dge.inpe.br)

B. T. Tsurutani, Jet Propulsion Laboratory (JPL), California Institute of Technology, Pasadena, CA 91109, USA.